

# Chemical Characterization of *Toona sinensis* Seeds and their Ameliorating Diabetic Nephropathy by Suppressing Streptozotocin-induced Oxidative Stress and Renal Fibrosis in Rats

Lulu Xuan<sup>1</sup>, Rongshen Wang<sup>1</sup>, Yan Lu<sup>1</sup>, Hongxia Zhang<sup>2</sup>, Chunzhen Zhao<sup>1</sup>, Xiaoxiao Liu<sup>1</sup>, Wenxian Jiang<sup>1</sup>, Xiaohong Wang<sup>1</sup>, Wanzhong Li<sup>1\*</sup>

<sup>1</sup>School of Pharmacy, Weifang Medical University, Weifang 261053, P. R. China, <sup>2</sup>Department of Clinic Pathology, Weifang Medical University, Weifang 261053, P. R. China

## ABSTRACT

The current study explored phytochemical constituents of fraction A (Fr. A) of *n*-BuOH extract of *Toona sinensis* seeds and evaluated protective effects of the corresponding fraction on diabetic nephropathy (DN). Kaempferol, quercetin, myricitrin, and rutin were isolated from Fr. A using silica gel column and preparative middle pressure liquid chromatography, the chemical structures of which were elucidated based on nuclear magnetic resonance and comparison with those reported in the literature. Myricitrin was first obtained from the genus *Toona*. Furthermore, Fr. A was further investigated to define pharmacological activity with ameliorating DN. Fr. A showed stronger inhibitory activity against high-glucose-stimulated rat glomerular mesangial cells proliferation *in vitro*. Fr. A could ameliorate significantly streptozotocin-induced DN rats by suppressing renal dysfunction and injury, oxidative stress, and transforming growth factor beta 1, connective tissue growth factor, and collagen IV expression levels *in vivo*, especially in the DN + M group, indicating that Fr. A might serve as a potential pharmacological agent treating DN.

**Key words:** Diabetic nephropathy, Meliaceae, oxidative stress, phytochemistry, *Toona sinensis* (A. Juss.) Roem.

## INTRODUCTION

Diabetic nephropathy (DN) is one of the most devastating microvascular complications of diabetes mellitus (DM), which is the primary cause of end-stage renal disease.<sup>[1]</sup> Existing evidence confirms that hyperglycemia is the primary pathogenetic factor for DN, which leads to increase oxidative stress (OS) and extracellular matrix (ECM) accumulation, thereby promoting the progress of DN.<sup>[2]</sup> Therefore, identifying effective agents that inhibit OS and ECM accumulation may be of great importance for treating DN. A number of natural products for ameliorating DN, including flavonoids,<sup>[3]</sup> phenols,<sup>[4]</sup> and triterpenoids,<sup>[5]</sup>

have been isolated from Chinese medicinal herbs. In our continuous efforts to identify potential compounds from Chinese medicinal herbs that treat DN, we found that the *n*-BuOH extract of *Toona sinensis* (A. Juss.) Roem. seeds had excellent protective effects on DN rats.<sup>[6]</sup>

*T. sinensis*, belonging to the Meliaceae family, is widely distributed in East and Southeast Asia.<sup>[7]</sup> It has a long history of more than 2000 years and is used to treat gastric ulcers, enteritis, dysentery, cerebrovascular, and cardiovascular diseases in China.<sup>[8]</sup> Modern pharmacological studies have revealed that the constituents of *T. sinensis* seeds include terpenoids, flavonoids, phenylpropanoids, and

### Address for correspondence:

Wanzhong Li, School of Pharmacy, Weifang Medical University, Weifang 261053, P. R. China; Xiaohong Wang, School of Pharmacy, Weifang Medical University, Weifang 261053, P. R. China.

© 2020 The Author(s). This open access article is distributed under a Creative Commons Attribution (CC-BY) 4.0 license.

anthraquinones, all of which can be applied for antitumor, antioxidation, and anticoagulation effects, decrease blood glucose, neuroinflammation, and other diseases.<sup>[9-11]</sup> *T. sinensis* seeds *n*-BuOH extract alleviates endothelial inflammation of DN and improves OS damage induced by high glucose (HG) in rat glomerular mesangial cells (GMCs).<sup>[12,13]</sup> Thus, it is believed that the active fractions isolated from the *n*-BuOH extract of *T. sinensis* seeds can potentially treat DN.

To date, the chemical constituents with ameliorating DN effects are still unknown from fraction A (Fr. A) of *n*-BuOH extract of *T. sinensis* seeds. As a result, the phytochemical analysis of Fr. A was also carried out and this study evaluated the ability of Fr. A to ameliorate streptozotocin (STZ)-induced DN rats by suppressing renal dysfunction and injury, OS, and transforming growth factor beta 1 (TGF- $\beta$ 1), connective tissue growth factor (CTGF), and collagen IV (Col IV) expression levels *in vivo*.

## MATERIALS AND METHODS

### General experimental procedures

The nuclear magnetic resonance (NMR) spectra were recorded using Bruker AV 500 MHz spectrometer (Bruker, Fällanden, Switzerland). Column chromatography was performed using silica gel (200–300 mesh, Branch of Qingdao Haiyang Chemical Co., Ltd., Qingdao, P.R. China). LiChroprep RP-18 gel (40–60  $\mu$ m) was purchased from Merck KGaA (Darmstadt, Germany). Thin-layer chromatography (TLC) was performed with pre-coated silica gel GF 254 glass plates (200  $\times$  200 mm, Branch of Qingdao Haiyang Chemical Co., Ltd.). All other chemicals and solvents were analytical grade and used without further purification.

### Plant material

*T. sinensis* seeds were collected by the Jinan Shengke Technology Company (Jinan, China) and identified by Prof. Chongmei Xu. A voucher specimen (voucher number: WF-YXY-TS1507) has been deposited at the Pharmacognosy Laboratory of the School of Pharmacy, Weifang Medical University.

### Preparation of plant extract

*T. sinensis* seeds were extracted with EtOH, filtered, and concentrated to dryness under reduced pressure. The dried crude extracts were suspended in distilled water. The suspension was partitioned with petroleum ether, EtOAc, and *n*-BuOH, sequentially. The *n*-BuOH extract was separated by silica gel column chromatography with gradient elution consisting of EtOAc and MeOH. The eluate was combined according to TLC to produce four fractions, named Fr. A-D, respectively.

### Screening of active fractions

GMCs (Boster Biological Technology Co. Ltd., Wuhan, China) in DMEM with 10% fetal bovine serum cultured for

24 h to allow cells to attach and incubated with 5.6 mmol/L glucose or 25 mmol/L glucose with Fr. A-D for 48 h. Cell viability was determined using [3-(4, 5-dimethylthiazol-2-yl)-2, 5-diphenyltetrazolium] method.<sup>[14]</sup> The absorbance was read at 490 nm by microplate reader. The half-maximal inhibitory concentration (IC<sub>50</sub>) values are reported as best fit value after normalization of data.

### Investigation of lipoidal compounds

The chemical composition of the Fr. A was characterized and identified by gas chromatography–mass spectrometry (GC–MS). ADB-5 quartz capillary column (30 m  $\times$  0.25 mm, 0.25  $\mu$ m) was used for analysis. Fr. A was injected at an injector temperature of 280°C. The temperature was gradually increased from 60 to 100°C at a rate of 3.5°C/min with 5 min holding time, and then to 200°C at a rate of 8°C/min for 5 min, and then to 280°C at a rate of 15°C/min with 15 min isothermal. Helium was used as the carrier gas at a flow rate of 1.2 mL/min. Mass spectra were taken at 70 eV. The ion source was EI at 280°C. Moreover, the transmission line temperature was 280°C. The mass range was set from 50 to 650 amu. The solvent delay was 6 min and total time was 69 min. The compounds were identified by comparison of their mass spectra from the NIST library.

### Isolation and characterization of compounds 1-4

Fr. A was separated chromatographically using silica gel and eluted with a gradient of CH<sub>2</sub>Cl<sub>2</sub> and MeOH to give five subfractions (Fr. A1-A5). Fr. A2 was separated by octadecylsilyl (ODS) and eluted with MeOH and H<sub>2</sub>O to give three subfractions (Fr. A21-A23). Fr. A22 was separated by ODS and eluted with MeOH and H<sub>2</sub>O to give compounds **1** and **2**. Fr. A3 was separated ODS and eluted with MeOH and H<sub>2</sub>O to give six subfractions (Fr. A31-A36). Fr. A34 was separated chromatographically using silica gel and eluted with CH<sub>2</sub>Cl<sub>2</sub> and MeOH to give compounds **3** and **4**.

### Animals

Male Wistar rats weighing 180–200 g were provided by the Center for Animal Testing of Shandong Lukang Drugs Group Limited and allowed to adapt to their new location for 1 week. The experimental protocols followed the institutional ethical guidelines for the care of laboratory animals of Weifang Medical University. All efforts were made to minimize animal suffering and to reduce the number of animals used. The animals received humane care throughout the study period.

### Induction of experimental diabetes

Experimental diabetes was induced in overnight fasted rats by a single intraperitoneal (i.p.) injection of 60 mg/kg body weight (BW) with STZ (STZ; Sigma, St. Louis, MO, USA) dissolved in 0.1 M citrate buffer (pH 4.5). Three days after the STZ injection, tail vein blood glucose concentration was measured to confirm the induction of DM, and their blood

glucose levels were within 16.7–25.0 mM. The rats were fed until their urine protein content was over 20 µg/mL.<sup>[15]</sup>

### Experimental design

Experimental animals were divided into five groups, each group consists of six rats, as below: Group 1: Normal control (NC) group rats administered with normal saline. Group 2: DN group rats administered with normal saline. Group 3: DN + L rats treated with Fr. A at 25 mg/kg BW. Group 4: DN + M treated with Fr. A at 50 mg/kg BW. Group 5: DN + H rats treated with Fr. A at 100 mg/kg BW. The Fr. A treatment was carried out by intragastric infusion for 8 weeks.

### Sample collection and preparation

After the end of the experiment, the rats were collected 24 h urine output (UO). Then, the rats were subjected to fasting for 12 h and weighed. Tail vein blood was obtained for detecting fasting blood glucose. The rats were anaesthetized and the blood samples were collected by intracardiac puncture. The kidneys were dissected, weighed, and rinsed with cold saline, and the left renal cortex was kept with glutaraldehyde for ultramicroscopic observation. The remaining portion of the left kidney was used for morphology observation and immunohistochemical detection. The right kidney was homogenized and centrifuged, and the supernatant obtained for further study.

### Biochemical analysis

The levels of UO, urinary protein excretion (UPE), urine creatinine (UCr), serum creatinine (SCr), blood urea nitrogen (BUN), malondialdehyde (MDA), superoxide dismutase (SOD), nitric oxide (NO), catalase (CAT), and glutathione peroxidase (GSH-px) in renal cortex were detected using commercially assay kits (Jiancheng Bioengineering Institute, Nanjing, China) following the manufacturer's instructions.

### Histopathological assessment

The kidney tissues were embedded in paraffin and slices were taken. The sections were stained with hematoxylin-eosin (HE), Masson's trichrome (Masson), periodic acid Schiff (PAS), and periodic acid-silver methenamine (PASM). The sections were examined under light microscopy at 400 × for pathological observations. The photos were analyzed with Image-Pro Plus 6.3 analyzing software (Media Cybernetics, Bethesda, USA). The sample slices were randomly selected to calculate the integral optical density.<sup>[16]</sup> Moreover, the prepared samples for ultrastructural observation under transmission electron microscope (TEM, H600A-2, Hitachi, Japan). The images were amplified 5000× and measured by an image analysis system.

### Immunohistochemistry analysis

Samples were dewaxed into water and rinsed with phosphate-buffered saline. After H<sub>2</sub>O<sub>2</sub> was added, they were incubated at

37°C for 30 min. Primary antibodies anti-TGF-β1 (ab92486, 1:100), anti-Col IV (ab6586, 1:100), and anti-CTGF (ab6992, 1:1000) and β-actin (ab8227) were obtained from Abcam Biotechnology Co., Ltd. (Shanghai, China). The samples were incubated with antibodies at 37°C in normal goat serum at 4°C overnight. Then, the secondary antibodies were added and incubated the slides at 37°C for 45 min. Immunostained tetrahydrate was observed using diaminobenzidine, and the slides were counterstained with hematoxylin. The immunoreactivity was analyzed by measuring the percentage of positive staining at 400× using computer-aided image analysis software.

### Real-time polymerase chain reaction (RT-PCR)

Total RNA from the renal cortex homogenate was isolated using Trizol reagent and quantified by measuring the absorbance at 260 nm. RNA quality was determined by measuring the 260/280 ratio.<sup>[17]</sup> Aliquots of 40 ng of total RNA samples were subjected to RT-PCR. Each reaction mix contained the following: 100 ng RNA, 100 ng primer, 12.5 µL 2 × PCR buffer, 2.0 µL RT mix, and DEPC-H<sub>2</sub>O to 25 µL. The following conditions were used: For reverse transcription, 15 min at 37°C; for the PCR initial activation step, 30 min at 95°C; and for amplification, 5 s at 95°C, 30 s at 60°C, and 30 s at 72°C, for 40 cycles. Changes in mRNA expression level were calculated following normalization with β-actin. Primer oligonucleotide sequences for TGF-β1, CTGF, and Col IV are shown in Table 1.

### Western blot

Total protein quantification was performed in kidney tissue using the Bradford assay method.<sup>[3]</sup> The renal cortex was lysed with RIPA lysate and the protein content was measured using a BCA protein assay kit. Then, 100 µg of the electrophoresis samples was applied to SDS-PAGE, transferred to PVDF membranes, incubated with 5% skim milk powder dissolved in Tris-buffered saline with Tween 20 for 1 h, and incubated with antibodies against TGF-β1, CTGF, Col IV, and β-actin (all 1:1000) overnight at 4°C. Bound antibody was incubated with horseradish peroxidase conjugated anti-rabbit IgG (1:5000) for 2 h. The signals were detected with a chemiluminescence system. Immunoreactive bands were quantitatively analyzed by AlphaView software (FluorChem Q, USA).

### Statistical analysis

Statistical differences between two groups were analyzed by the *t*-test and differences between multiple groups of data were analyzed by one-way ANOVA with prism software (GraphPad, San Diego, CA) and expressed as the mean ± SD of three independent experiments.\**P* < 0.01 compared with NC and # *P* < 0.05 and ## *P* < 0.01 compared with DN which were considered statistically significant.

**Table 1:** Primer sequences used for real-time PCR reactions

Primer set	Sense primer 5prime	Antisense primer 5prime
TGF- $\beta$ 1	TGGACCGCAACAACGCAATC	AAGACAGCCACTCAGGCGTATCAG
CTGF	AGCCTGTCAAGTTTGAGCTTTCTGG	CAGTTGTAATGGCAGGCACAGGTC
Col IV	GATTGTGGTGGCTCTGGCTGTG	CAGGAAGTCCAGGTTCTCCAGCAT
$\beta$ -actin	TGTTGTCCCTGTATGCCTCTGGTC	GTCACGCACGATTTCCCTCTCA

## RESULTS AND DISCUSSION

### Active fractions screening by HG-induced GMCs proliferation *in vitro*

To seek out the effective fractions with ameliorating DN activity, Fr. A-D inhibited the proliferation of GMCs stimulated by HG within non-toxic concentrations. As shown in Figure 1, all fractions of the *n*-BuOH extract of *T. sinensis* seeds were active toward GMCs proliferation. Among of them, Fr. A showed better activity than Fr. B-D comparing with IC<sub>50</sub>, thus, Fr. A was selected for subsequent experiments.

### Investigation of lipoidal compounds from Fr. A

Twelve lipoidal compounds were identified from Fr. A using GC-MS analysis according to the presence of 12 peaks [Figure 2]. The major compounds were identified as hexamethylcyclotrisiloxane, *n*-methylformanilide, tetradecane, tributyl phosphate, conhydrine, 4-amino-6-ethoxy-1, 3, 5-triazine-2-carbohydrazide, hexadecanoic acid, palmitic acid *n*-butyl ester, methyl linoleate, *n*-[24-oxo-3 $\alpha$ , 7 $\alpha$ , 12 $\alpha$ -tris(trimethylsiloxy)-5 $\beta$ -cholan-24-yl] glycine methyl ester, cholesteryl chloroformate, and phorbol 12, 13-didecanoate. The retention time, molecular formula, and molecular weight of these compounds are shown in Table 2.

### Identification of compounds 1-4 from Fr. A

Ameliorating DN activity depends on the chemical constituents of Fr. A, which are further investigated to describe characterization of major component. Four known compounds were isolated from the Fr. A of *n*-BuOH extract of *T. sinensis* seeds using silica gel column and preparative middle pressure liquid chromatography. The chemical structures were identified as kaempferol (**1**),<sup>[18]</sup> quercetin (**2**),<sup>[19]</sup> myricitrin (**3**),<sup>[20]</sup> and rutin (**4**) [Figure 3],<sup>[21]</sup> which were elucidated based on 1D NMR and comparison with those reported in the literature. It should be noted that compound **3** was obtained from the genus *Toona* for the 1<sup>st</sup> time.

**Kaempferol (1):** <sup>1</sup>H-NMR (500 MHz, methanol-*d*<sub>4</sub>)  $\delta_{\text{H}}$  8.08 (2H, d,  $J = 8.9$  Hz, H-2', 6'), 6.90 (2H, d,  $J = 8.9$  Hz, H-3', 5'), 6.39 (1H, d,  $J = 2.1$  Hz, H-6), 6.18 (1H, d,  $J = 2.1$  Hz, H-8); <sup>13</sup>C-NMR (125 MHz, methanol-*d*<sub>4</sub>)  $\delta_{\text{C}}$  177.4 (C-4), 165.6 (C-7), 162.5 (C-4'), 160.6 (C-5), 158.3 (C-9), 148.0 (C-2), 137.1 (C-3), 130.7 (C-3', 5'), 123.7 (C-1'), 116.3 (C-2', 6'), 104.5 (C-10), 99.3 (C-6), 94.5 (C-8).

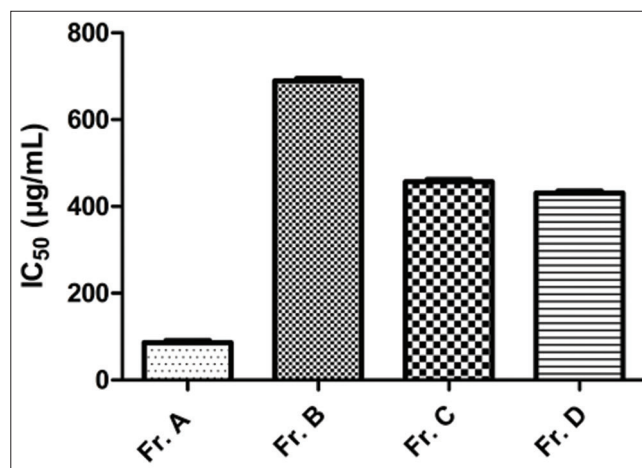


**Figure 1:** Effects of different fractions inhibited HG-induced glomerular mesangial cells proliferation *in vitro*

**Quercetin (2):** <sup>1</sup>H-NMR (500 MHz, methanol-*d*<sub>4</sub>)  $\delta_{\text{H}}$  7.73 (1H, d,  $J = 2.1$  Hz, H-2'), 7.63 (1H, dd,  $J = 8.5, 2.1$  Hz, H-6'), 6.88 (1H, d,  $J = 8.5$  Hz, H-5'), 6.38 (1H, d,  $J = 2.1$  Hz, H-6), 6.18 (1H, d,  $J = 2.1$  Hz, H-8); <sup>13</sup>C-NMR (125 MHz, methanol-*d*<sub>4</sub>)  $\delta_{\text{C}}$  177.3 (C-4), 165.6 (C-7), 162.5 (C-9), 158.2 (C-2), 148.8 (C-5), 148.0 (C-4'), 146.2 (C-3'), 137.2 (C-3), 124.1 (C-1'), 121.7 (C-6'), 116.2 (C-5'), 116.0 (C-2'), 104.5 (C-10), 99.2 (C-6), 94.4 (C-8).

**Myricitrin (3):** <sup>1</sup>H-NMR (500 MHz, methanol-*d*<sub>4</sub>)  $\delta_{\text{H}}$  6.95 (2H, s, H-2', 6'), 6.36 (1H, d,  $J = 2.1$  Hz, H-6), 6.20 (1H, d,  $J = 2.1$  Hz, H-8), 5.32 (1H, d,  $J = 1.7$  Hz, H-1''), 4.22 (1H, dd,  $J = 3.4, 1.7$  Hz, H-5''), 3.78 (1H, dd,  $J = 9.5, 3.4$  Hz, H-2''), 3.52 (1H, dd,  $J = 9.5, 6.1$  Hz, H-3''), 3.35 (1H, m, H-4''), 0.96 (3H, d,  $J = 6.2$  Hz, 6''-CH<sub>3</sub>); <sup>13</sup>C-NMR (125 MHz, methanol-*d*<sub>4</sub>)  $\delta_{\text{C}}$  179.7 (C-4), 165.9 (C-7), 163.3 (C-5), 159.5 (C-9), 158.5 (C-2), 146.9 (C-3', 5'), 137.9 (C-4'), 136.3 (C-3), 121.9 (C-1'), 109.6 (C-2', 6'), 103.7 (C-1'), 99.8 (C-6), 94.7 (C-8), 73.4 (C-4''), 72.1 (C-2'', C-3''), 71.9 (C-5''), 17.7 (C-6'').

**Rutin (4):** <sup>1</sup>H-NMR (500 MHz, methanol-*d*<sub>4</sub>)  $\delta_{\text{H}}$  7.67 (1H, d,  $J = 2.1$  Hz, H-2'), 7.63 (1H, dd,  $J = 8.4, 2.1$  Hz, H-6'), 6.87 (1H, d,  $J = 8.4$  Hz, H-5'), 6.40 (1H, d,  $J = 2.1$  Hz, H-6), 6.21 (1H, d,  $J = 2.1$  Hz, H-8), 5.11 (1H, d,  $J = 7.7$  Hz, H-1''), 4.52 (1H, d,  $J = 1.3$  Hz, H-1'''), 3.80-3.24 (sugar protons), 1.12 (3H, d,  $J = 6.2$  Hz, 6'''-CH<sub>3</sub>); <sup>13</sup>C-NMR (125 MHz, methanol-*d*<sub>4</sub>)  $\delta_{\text{C}}$  178.0 (C-4), 164.6 (C-7), 161.6 (C-5), 157.9

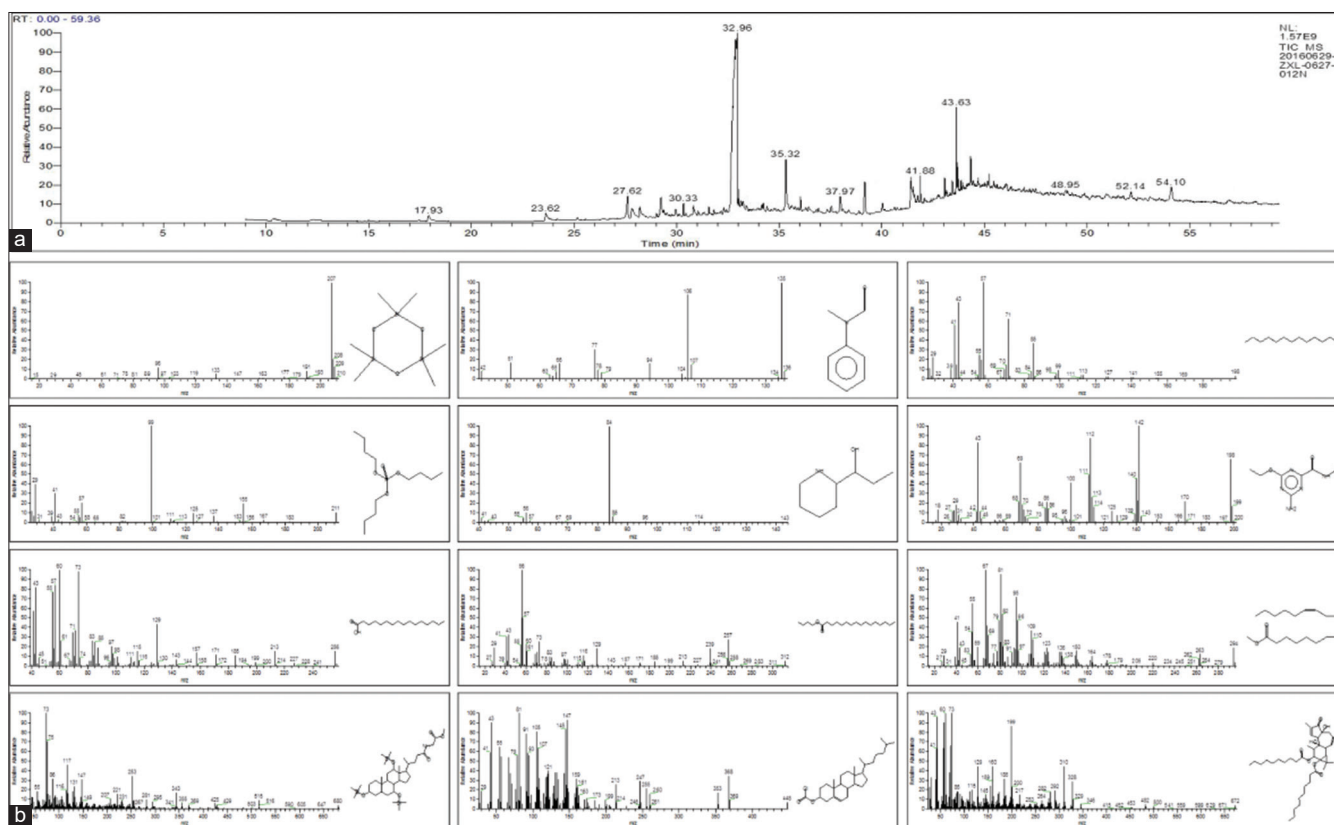


**Figure 2:** (a) Chromatogram showing peaks with retention time (X-axis, retention time; Y-axis, % intensity/% abundance). (b) Gas chromatography–mass spectrometry (GC–MS) analysis of the major compounds in fraction A

**Table 2:** The compounds of Fr. A and their retention time, molecular formulas, and molecular weights

No.	RT (min)	Name of the compounds	Molecular formula	Molecular weight
1	17.93	Hexamethylcyclotrisiloxane	C <sub>6</sub> H <sub>18</sub> O <sub>3</sub> Si <sub>3</sub>	222
2	23.62	<i>n</i> -Methylformanilide	C <sub>8</sub> H <sub>9</sub> NO	135
3	27.62	Tetradecane	C <sub>14</sub> H <sub>30</sub>	198
4	30.33	Tributyl phosphate	C <sub>12</sub> H <sub>27</sub> O <sub>4</sub> P	266
5	32.96	Conhydrine	C <sub>8</sub> H <sub>17</sub> NO	143
6	35.32	4-Amino-6-ethoxy-1,3,5-triazine-2-carbohydrazide	C <sub>6</sub> H <sub>10</sub> N <sub>6</sub> O <sub>2</sub>	198
7	37.97	Hexadecanoic acid	C <sub>16</sub> H <sub>32</sub> O <sub>2</sub>	256
8	41.88	Palmitic acid <i>n</i> -butyl ester	C <sub>20</sub> H <sub>40</sub> O <sub>2</sub>	312
9	43.63	Methyl linoleate	C <sub>19</sub> H <sub>34</sub> O <sub>2</sub>	294
10	48.95	<i>n</i> -[24-Oxo-3 $\alpha$ ,7 $\alpha$ ,12 $\alpha$ -tris(trimethylsiloxy)-5 $\beta$ -cholan-24-yl] glycine methyl ester	C <sub>36</sub> H <sub>69</sub> NO <sub>6</sub> Si <sub>3</sub>	695
11	52.14	Cholesteryl chloroformate	C <sub>28</sub> H <sub>45</sub> ClO <sub>2</sub>	449
12	54.10	Phorbol 12,13-didecanoate	C <sub>40</sub> H <sub>64</sub> O <sub>8</sub>	672

(C-2), 157.1 (C-9), 148.4 (C-4'), 144.5 (C-3'), 134.2 (C-3), 122.2 (C-6'), 121.7 (C-1'), 116.3 (C-5'), 114.7 (C-2'), 104.2 (C-10), 103.3 (C-1''), 101.0 (C-1'''), 98.5 (C-6), 93.5 (C-8), 76.8 (C-3''), 75.8 (C-5''), 74.3 (C-2''), 72.5 (C-4'''), 70.8 (C-4''), 70.7 (C-2'''), 70.0 (C-3'''), 68.3 (C-5'''), 67.2 (C-6''), 16.5 (C-6''').

### Fr. A relieved STZ-induced renal dysfunction and injury in DN rats

So as to confirm the effects of Fr. A on renal system of STZ-induced DN rats, the kidney index and renal functional parameters were determined. The BW and UCr of DN rats were appreciably decreased, but the kidney hypertrophy (kidney weight/BW [KW/BW]), serum glucose, UO, UPE,

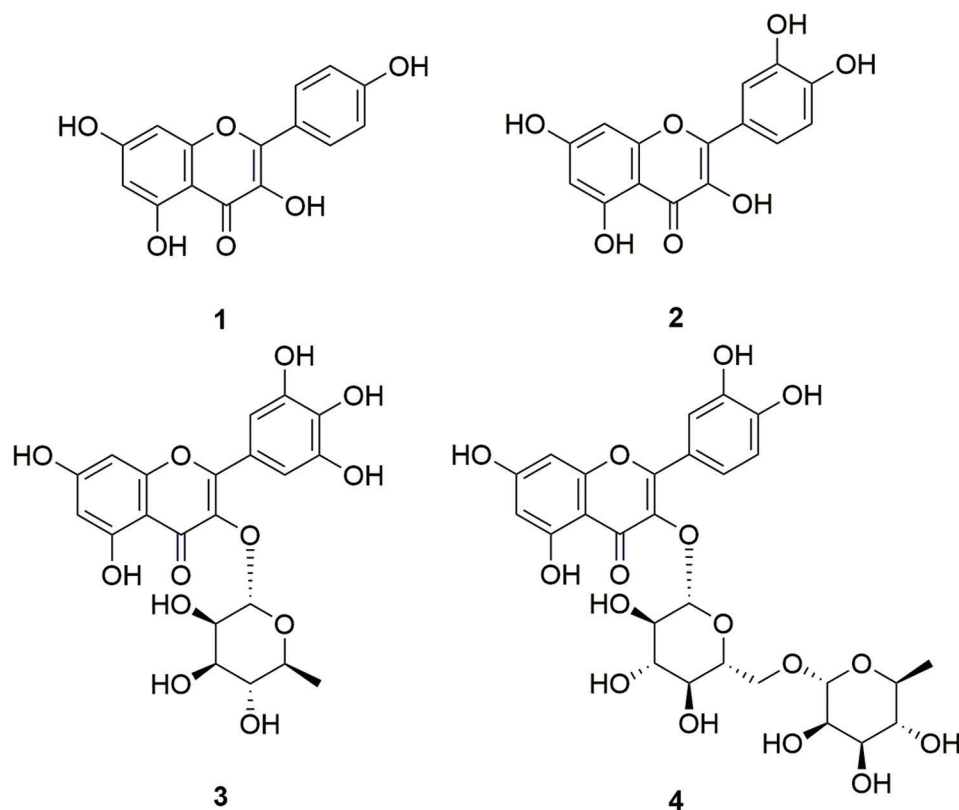


**Figure 3:** The structures of compounds 1-4 isolated from the fraction A from the *n*-BuOH extract of *Toona sinensis* seeds

SCr, and BUN in DN rats were significantly increased compared to the NC group, indicating the occurrence of renal hypertrophy in the DN group. However, compared to the DN group, treatment with Fr. A significantly increased the BW [Figure 4a] and UCr [Figure 4g], meanwhile decreased KW/BW [Figure 4b], serum glucose [Figure 4c], UO [Figure 4d], UPE [Figure 4e], SCr [Figure 4f], and BUN [Figure 4h] ameliorating renal functional parameters in STZ-induced DN rats, especially in the DN + M group.

In addition, to assess the kidney tissue injury, ECM accumulation was determined by HE, Masson, PAS, PASM, and TEM staining. The results showed that the HE, Masson, PAS, and PASM staining were increased in STZ-induced DN rats compared with the NC group, whereas Fr. A treatment markedly decreased HE, Masson, PAS, and PASM staining in DN rats [Figure 5a]. Similarly, the results of TEM also indicated that Fr. A mitigated STZ-induced renal dysfunction and injury in DN rats [Figure 5b].

#### Fr. A alleviated STZ-induced renal cortex OS in DN rats

To evaluate the effects of Fr. A on OS injury in DN, the levels of MDA, SOD, NO, CAT, and GSH-px were measured. STZ treatment resulted in a significant increase of the levels of MDA and NO, and a remarkable decrease of the levels of SOD, CAT, and GSH-px in renal cortex of rats, indicating a

rise of OS in DN rats. However, Fr. A treatment dramatically reduced the levels of MDA [Figure 6a] and NO [Figure 6c] and improved SOD [Figure 6b], CAT [Figure 6d], and GSH-px [Figure 6e] levels in renal cortex of STZ-induced DN rats.

OS is regarded as one of the major risk factors for the development of DN.<sup>[22]</sup> MDA can reflect the content of oxygen-free radicals in tissue and NO has been implicated in the development of DN and is associated with increased hyperfiltration and microalbuminuria.<sup>[23,24]</sup> SOD and GSH-px are enzymes in mitochondria that play an important role in antioxidant defense. Decreased activity of CAT, a protector of cell membranes and cellular constituents from oxidative damage, may be due to the overproduction of reactive oxygen species.<sup>[25]</sup> Our research shows that Fr. A has the characteristics of an antioxidant *in vivo* and this could be of benefit for protection in DN. This suggested that suppression of OS is an effective way to prevent DN.

#### Fr. A inhibited STZ-induced TGF- $\beta$ 1, CTGF, and Col IV expression levels in DN rats

To investigate the interaction between Fr. A and TGF- $\beta$ 1, CTGF, and Col IV, the influence of Fr. A on expression of TGF- $\beta$ 1, CTGF, and Col IV levels was detected by immunohistochemistry analysis, RT-PCR, and Western blot. The results indicated that STZ markedly increased the

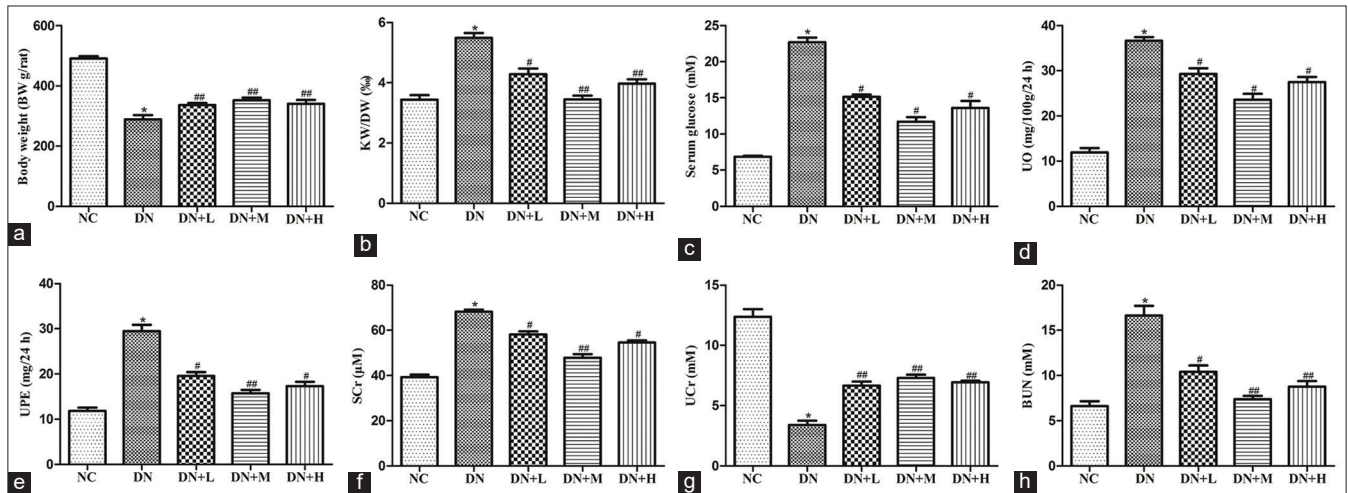


**Figure 4:** (a-h) Effects of fraction A on streptozotocin-induced renal dysfunction and injury in diabetic nephropathy (DN) rats. The results were presented as mean ± standard deviation ( $n = 6$ ). \* $P < 0.01$ , compared with normal control group; # $P < 0.05$  and ## $P < 0.01$ , compared with DN group

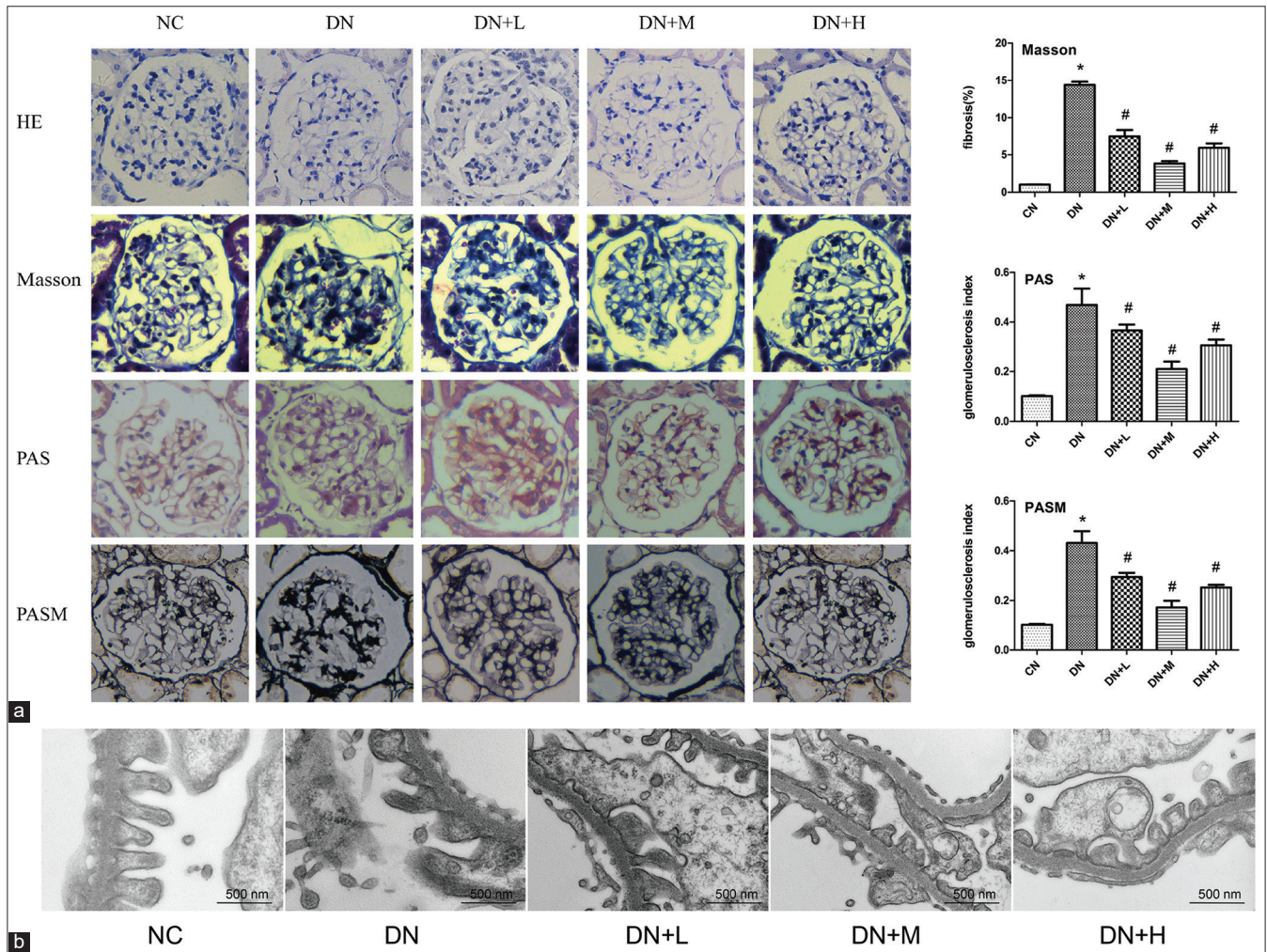


**Figure 5:** (a) Histopathological changes in the kidneys of diabetic nephropathy (DN) rats with fraction A treatment were stained with hematoxylin-eosin, Masson's trichrome (Masson), periodic acid Schiff (PAS), and periodic acid-silver methenamine (PASM) staining (400×). Masson, PAS, and PASM staining were determined semi-quantitatively as described above. Data were reported as mean ± standard deviation ( $n = 6$ ). \* $P < 0.01$ , compared with normal control group; # $P < 0.05$ , compared with DN group. (b) Structural changes were observed in renal ultrastructures of DN rats by transmission electron microscope (TEM, 5000×)

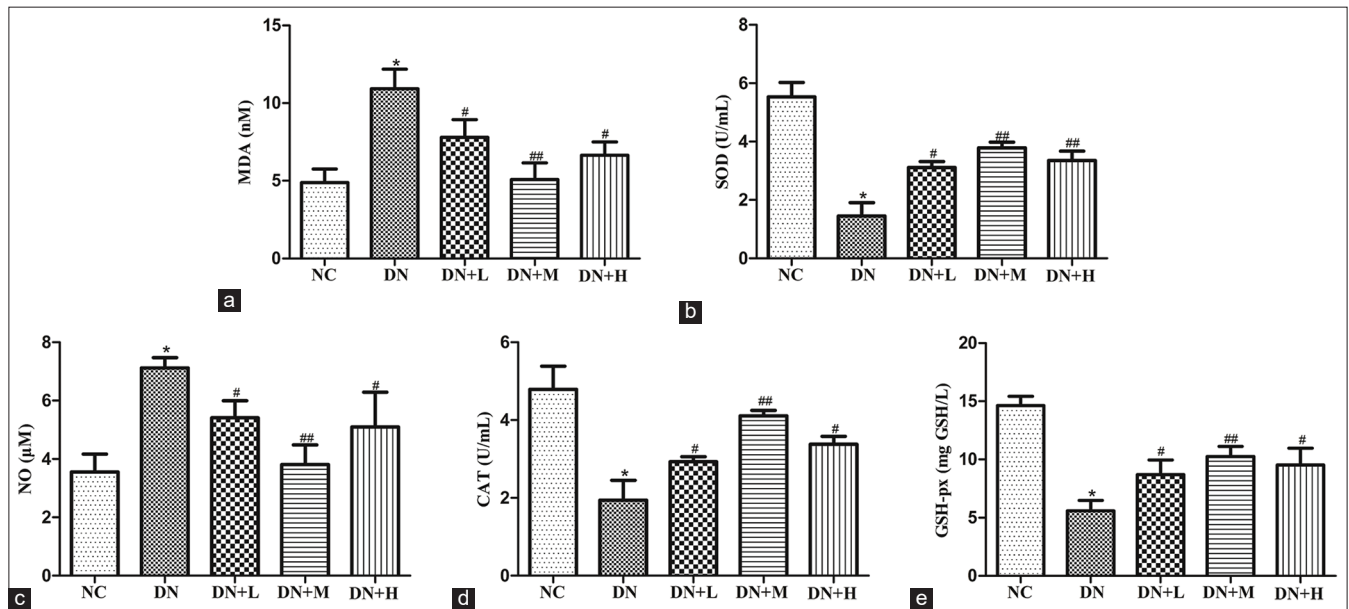


**Figure 6:** (a-e) Effects of fraction A on streptozotocin-induced renal cortex oxidative stress in diabetic nephropathy (DN) rats. The results are presented as mean  $\pm$  standard deviation ( $n = 6$ ). \* $P < 0.01$ , compared with normal control group; # $P < 0.05$  and ## $P < 0.01$ , compared with DN group

expression of TGF- $\beta$ 1, CTGF, and Col IV levels. However, Fr. A significantly restrained the expression of TGF- $\beta$ 1, CTGF, and Col IV levels in STZ-induced DN rats [Figure 7], suggesting that Fr. A repressed TGF- $\beta$ 1, CTGF, and Col IV expression levels in STZ-induced DN rats.

TGF- $\beta$ 1 is responsible for moderating glomerulosclerosis and tubulointerstitial fibrosis by amplifying the synthesis of the ECM in DN.<sup>[26]</sup> Renal fibrosis can be activated by hyperglycemia-induced OS through the TGF- $\beta$ 1 pathway.<sup>[27]</sup> Collagen and hydroxyproline are considered the key markers of fibrosis.<sup>[28]</sup> The hyperglycemia that initially induces the increased expression of TGF- $\beta$ 1 results in the accumulation of Col IV. The activated TGF- $\beta$ 1/Smad signaling pathway induces the accumulation of ECM.<sup>[29]</sup> CTGF is considered a downstream mediator of TGF- $\beta$ 1 and a potent inducer of ECM in the fibrotic process.<sup>[30]</sup> Thus, the inhibition of TGF- $\beta$ 1 expression can aid in the prevention of DN by alleviating ECM accumulation. Furthermore, Fr. A decreased the levels of TGF- $\beta$ 1, CTGF, and Col IV expression at both the mRNA and protein levels in treated DN rats, which might be related to its attenuation of OS. Consequently, the possible mechanisms may be related to reducing hyperglycemia, decreasing urinary protein, improving renal function and structure, restraining OS, and inhibiting the expression of TGF- $\beta$ 1, CTGF, and Col IV.

Strong evidences were provided that Fr. A ameliorates STZ-induced DN rats by suppressing renal dysfunction and injury, OS, and TGF- $\beta$ 1, CTGF, and Col IV expression levels *in vivo*, indicating that Fr. A might be a beneficial agent for the prevention and treatment of DN. It is worth noting that

all experimental results show that the DN + M group is the optimal dose. In our continuous efforts to explore potential chemical constituents from the Fr. A of *n*-BuOH extract of *T. sinensis* seeds, kaempferol,<sup>[31]</sup> quercetin,<sup>[32]</sup> myricitrin,<sup>[33]</sup> and rutin<sup>[34]</sup> were defined, which all play a major role in improving DN.

## CONCLUSION

The results of this study demonstrated the Fr. A of *n*-BuOH extract of *T. sinensis* seeds as a mean of ameliorating DN agents for the 1<sup>st</sup> time and phytochemical evaluation confirmed the presence of kaempferol, quercetin, myricitrin, and rutin in Fr. A, which contributed to the positive ameliorating DN effect. However, further studies need to be carried out to verify whether the combination of compounds had synergistic inhibitory effect on various proteins or genes related to DN.

## CONFLICTS OF INTEREST

The authors declare that they have no conflicts of interest.

## FUNDING

This research was supported by Natural Science Foundation of Shandong Province (ZR2018MH040 and ZR2017LH075), Shandong Science and Technology Research Project of Traditional Chinese Medicine (2015227 and 2017209), National Nature Science Foundation of China (81274049), and Science and Technology Development Project of Weifang City (2017YX062).

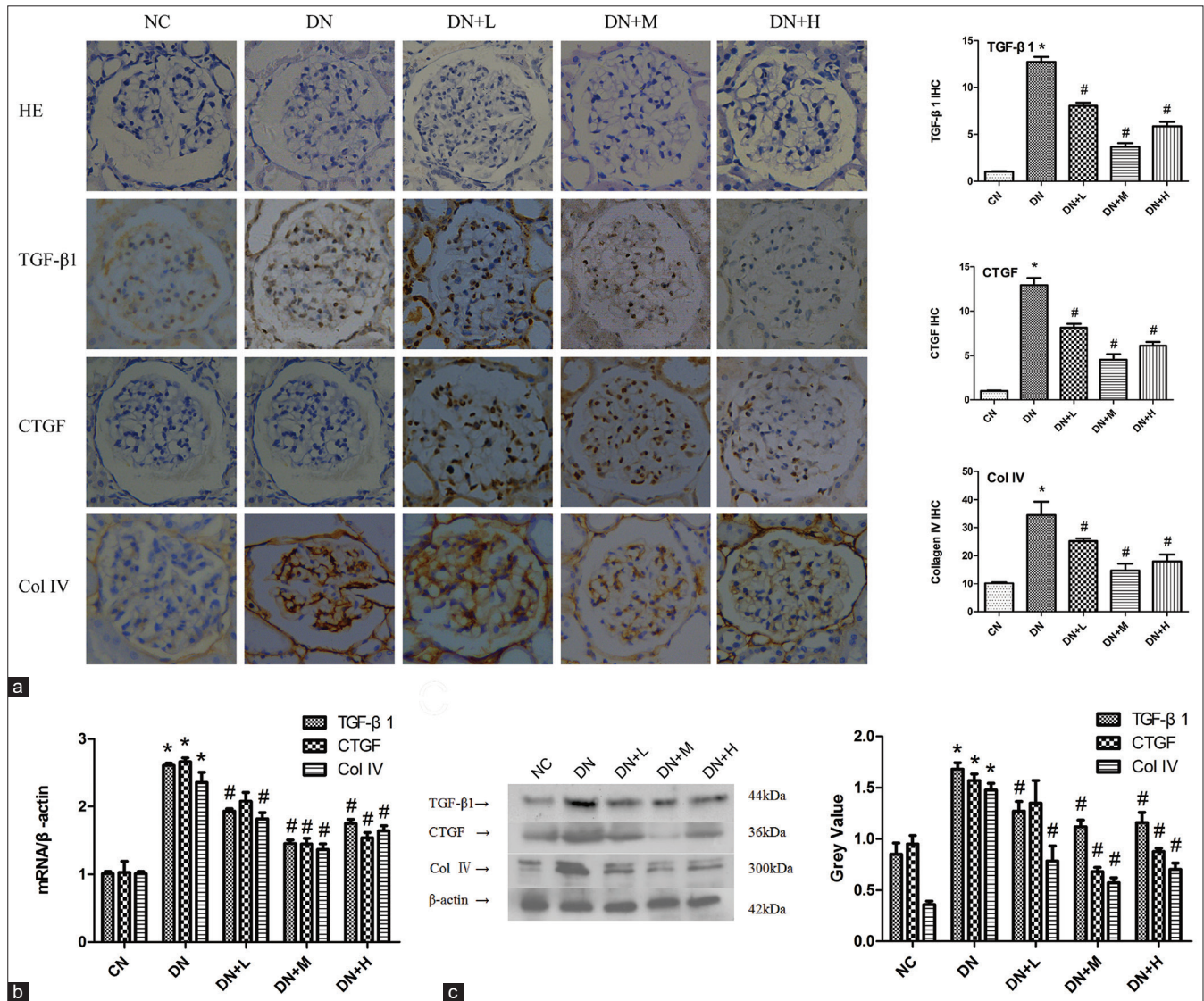


**Figure 7:** (a) Immunohistochemical photograph (400×) and semi-quantitative analysis of transforming growth factor beta 1 (TGF-β1), connective tissue growth factor (CTGF), and collagen IV (Col IV) in kidneys of DN rats with fraction A (Fr. A) treatment were indicated. Data were reported as means ± standard deviation (SD) (n = 6). (b) mRNA level changes of TGF-β1, CTGF, and Col IV in kidneys of DN rats with Fr. A treatment were presented as mean ± SD (n = 6). (c) Effects of Fr. A on TGF-β1, CTGF, and Col IV protein expression in kidneys of DN rats with Fr. A treatment were examined by Western blot. The results are presented as mean ± SD (n = 6). \*P < 0.01, compared with NC group; #P < 0.05, compared with DN group

## AUTHORS' CONTRIBUTIONS

Rongshen Wang and Xiaoxiao Liu carried out the extract, isolation, purification, and running the laboratory work. Lulu Xuan, Yan Lu, Hongxia Zhang, Chunzhen Zhao, and Wenxian Jiang contributed to biological studies. Xiaohong Wang and Wanzhong Li contributed equally to this paper on structural determination and writing this paper.

## REFERENCES

- Xie Z, Zhong L, Wu Y, Wan X, Yang H, Xu X, *et al.* Carnosic acid improves diabetic nephropathy by activating Nrf2/ARE and inhibition of NF-κB pathway. *Phytomedicine* 2018;47:161-73.
- Xiang H, Xue W, Wu X, Zheng J, Ding C, Li Y, *et al.* FOXP1 inhibits high glucose-induced ECM accumulation and oxidative stress in mesangial cells. *Chem Biol Interact* 2019;313:108818.
- Jiang W, Wang R, Liu D, Zuo M, Zhao C, Zhang T, *et al.* Protective effects of kaempferitrin on advanced glycation end products induce mesangial cell apoptosis and oxidative stress. *Int J Mol Sci* 2018;19:3334.
- Bao L, Li J, Zha D, Zhang L, Gao P, Yao T, *et al.* Chlorogenic acid prevents diabetic nephropathy by inhibiting oxidative stress and inflammation through modulation of the Nrf2/HO-1 and NF-κB pathways. *Int Immunopharmacol* 2018;54:245-53.
- Liu D, Wang RS, Xuan LL, Wang XH, Li WZ. Two new

- apotirucallane-type triterpenoids from the pericarp of *Toona sinensis* and their ability to reduce oxidative stress in rat glomerular mesangial cells cultured under high-glucose conditions. *Molecules* 2020;25:801.
6. Li WZ, Wang XH, Zhang HX, Mao SM, Zhao CZ. Protective effect of the n-butanol *Toona sinensis* seed extract on diabetic nephropathy rat kidneys. *Genet Mol Res* 2016;15:15017403.
  7. Wang R, Zuo M, Ding S, Liu B, Meng C, Song B, *et al.* Recovery of immune activity by administration of polysaccharides of *Toona sinensis* and its characterization of major component. *Nat Prod Res* 2020;1-5.
  8. Peng W, Liu YJ, Hu M, Zhang M, Yang J, Liang F, *et al.* *Toona sinensis*: A comprehensive review on its traditional usages, phytochemistry, pharmacology and toxicology. *Rev Bras Farmacogn* 2019;29:111-24.
  9. Li W, Ding J, Zhang X, Tian J. Research progress on chemical composition, extraction methods and biological activities of *Toona sinensis* Roem. *Qilu Pharm Aff* 2012;31:37-9.
  10. He Z, Lin L. Research progress in chemical constituents and pharmacological action of *Toona sinensis* seeds. *J Gansu College of TCM* 2013;30:64-6.
  11. Zhuang W, Chen C, Ma Y, Song L, Lyu E, Fu W. Polyphenols from *Toona sinensis* seeds alleviate neuroinflammation in rats with Parkinson's disease via inhibiting p38MAPK signaling pathway. *Xi Bao Yu Fen Zi Mian Yi Xue Za Zhi* 2019;35:794-9.
  12. Guo Y, Zhong Y, Zheng X, Yu L, Li W, Zhang H. Extract of *Toona sinensis* improves glomerular endothelial cell inflammation in DN and its potential mechanism. *Nat Prod Res Dev* 2019;31:55-60.
  13. Zhong Y, Hu S, Wang T, Zhang Y, Li W, Yu L, *et al.* N-butyl alcohol extract of *Toona sinensis* attenuates the oxidative stress of glomerular endothelial cells induced by high glucose through activating Nrf2. *Chin J Histochem Cytochem* 2019;28:197-203.
  14. Liu S, Li X, Gao J, Liu Y, Shi J, Gong Q. Icariside II, a phosphodiesterase-5 inhibitor, attenuates beta-amyloid-induced cognitive deficits via BDNF/TrkB/CREB signaling. *Cell Physiol Biochem* 2018;49:985.
  15. Yuan P, Xue H, Zhou L, Qu L, Li C, Wang Z, *et al.* Rescue of mesangial cells from high glucose-induced over-proliferation and extracellular matrix secretion by hydrogen sulfide. *Nephrol Dial Transpl* 2011;26:2119-26.
  16. Border WA, Okuda S, Languino LR, Sporn MB, Ruoslahti E. Suppression of experimental glomerulonephritis by antiserum against transforming growth factor beta 1. *Nature* 1990;346:371-4.
  17. Giribabu N, Karim K, Kilari EK, Salleh N. *Phyllanthus niruri* leaves aqueous extract improves kidney functions, ameliorates kidney oxidative stress, inflammation, fibrosis and apoptosis and enhances kidney cell proliferation in adult male rats with diabetes mellitus. *J Ethnopharmacol* 2017;205:123-37.
  18. Zhang ZL, Zuo YM, Xu L, Qu XS, Luo YM. Studies on chemical components of flavonoids in aerial part of *Saururus chinensis*. *Chin Tradit Herb Drugs* 2011;42:1490-3.
  19. Ye C, Jin M, Jin C, Wang R, Wang J, Zhang Y, *et al.* Two novel flavonoids from the leaves of *Rhododendron dauricum* L. with their inhibition of TNF- $\alpha$  production in LPS-induced RAW 264.7 cells. *Nat Prod Res* 2019;1-9.
  20. Liao HW, Liu EG, Wang DY. Chemical constituents of the bark of *Myrica rubra*. *Cent South Pharm* 2006;3:196-9.
  21. Hamad KM, Sabry MM, Elgayed SH, El Shabrawy AR, El-Fishawy AM, Jaleel GA. Anti-inflammatory and phytochemical evaluation of *Combretum aculeatum* Vent growing in Sudan. *J Ethnopharmacol* 2019;242:112052.
  22. Kashihara N, Haruna Y, Kondeti VK, Kanwar YS. Oxidative stress in diabetic nephropathy. *Curr Med Chem* 2010;17:4256-69.
  23. Joshi MS, Mihm MJ, Cook AC, Schanbacher BL, Bauer JA. Alterations in connexin 43 during diabetic cardiomyopathy: Competition of tyrosine nitration versus phosphorylation. *J Diabetes* 2015;7:250-9.
  24. Noriega-Cisneros R, Cortés-Rojo C, Manzo-Avalos S, Clemente-Guerrero M, Calderón-Cortés E, Salgado-Garciglia R. Mitochondrial response to oxidative and nitrosative stress in early stages of diabetes. *Mitochondrion* 2013;13:835-40.
  25. Giacco F, Brownlee M. Oxidative stress and diabetic complications. *Circ Res* 2010;107:1058-70.
  26. Pal PB, Sinha K, Sil PC. Mangiferin attenuates diabetic nephropathy by inhibiting oxidative stress mediated signaling cascade, TNF $\alpha$  related and mitochondrial dependent apoptotic pathways in streptozotocin-induced diabetic rats. *PLoS One* 2014;9:e107220.
  27. Zhao TT, Zhang HJ, Lu XG, Huang XR, Zhang WK, Wang H, *et al.* Chaihuang-Yishen granule inhibits diabetic kidney disease in rats through blocking TGF- $\beta$ /Smad3 signaling. *PLoS One* 2014;9:e90807.
  28. Zhai YP, Lu Q, Liu YW, Cheng Q, Wei YQ, Zhang F, *et al.* Over-production of nitric oxide by oxidative stress-induced activation of the TGF- $\beta$ 1/PI3K/Akt pathway in mesangial cells cultured in high glucose. *Acta Pharmacol Sin* 2013;34:507-14.
  29. Gagliardini E, Benigni A. Role of anti-TGF-beta antibodies in the treatment of renal injury. *Cytokine Growth Factor Rev* 2006;17:89-96.
  30. Nguyen TQ, Tarnow L, Jorsal A, Oliver N, Roestenberg P, Ito Y, *et al.* Plasma connective tissue growth factor is an independent predictor of end-stage renal disease and mortality in type 1 diabetic nephropathy. *Diabetes Care* 2008;31:1177-82.
  31. Sharma D, Gondaliya P, Tiwari V, Kalia K. Kaempferol attenuates diabetic nephropathy by inhibiting RhoA/Rho-kinase mediated inflammatory signaling. *Biomed Pharmacother* 2019;109:1610-9.
  32. Tang LX, Li K, Zhang Y, Li H, Li A, Xu Y, *et al.* Quercetin liposomes ameliorate streptozotocin-induced diabetic nephropathy in diabetic rats. *Sci Rep* 2020;10:2440.
  33. Ahangarpour A, Oroojan AA, Khorsandi L, Kouchak M, Badavi M. Antioxidant, anti-apoptotic, and protective effects of myricitrin and its solid lipid nanoparticle on streptozotocin-nicotinamide-induced diabetic nephropathy in type 2 diabetic male mice. *Iran J Basic Med Sci* 2019;22:1424-31.
  34. Ganesan D, Albert A, Paul E, Ananthapadmanabhan K, Andiappan R, Sadasivam SG. Rutin ameliorates metabolic acidosis and fibrosis in alloxan induced diabetic nephropathy and cardiomyopathy in experimental rats. *Mol Cell Biochem* 2020;471:41-50.

**How to cite this article:** Xuan L, Wang R, Lu Y, Zhang H, Zhao C, Liu X, Jiang W, Wang X, Li W. Chemical Characterization of *Toona sinensis* Seeds and their Ameliorating Diabetic Nephropathy by Suppressing Streptozotocin-induced Oxidative Stress and Renal Fibrosis in Rats. *Clin Res Diab Endocrinol* 2020;3(2):1-10.